Seasonal Climate Outlook for Africa

November–January, December–February and January–March 2026/27 · issued 27 October 2026 from the October 2026 initialisations

ACMAD objective forecast · rainfall and 2 m temperature

Key messages

Rainfall, December–February 2026/27. Above-normal rainfall is the most likely outcome over equatorial East Africa, at 60 to 70 % over Kenya, southern Somalia, northern Tanzania and Uganda. Below-normal rainfall is the most likely outcome over southern Africa, at 50 to 70 % over Botswana, Zimbabwe, Namibia, the South African interior, southern Angola and southern Mozambique. Below-normal rainfall is also the most likely outcome, at 50 to 70 %, over Cameroon, Gabon and the Congo coast. The Congo basin interior, Madagascar and about half of Angola, Zambia and northern Mozambique are left white: the forecast has no skill there in the 1991–2020 hindcast and no category is issued. The East African signal is strongest in November–January, at 70 to 90 %, and fades through January–March. The southern African signal holds through December–February and weakens in January–March.

Temperature, December–February 2026/27. Above-normal 2 m temperature is the most likely outcome over almost the whole continent. The probability is 80 to 90 % over Angola, Madagascar, Mozambique, Somalia, Tanzania, Zambia, the Congo basin and the Ethiopian highlands, 60 to 80 % over most other regions, and 40 to 60 % over Egypt, the Sahara and the Sahel. Over the Nile valley and the Lake Victoria basin no category reaches 50 %. Below-normal temperature leads at 40 to 50 % over northern Sudan and around Lake Victoria. Much of Mauritania and the western Sahara is left white for lack of hindcast skill.

The ocean. A strong El Niño is in place. The observed Niño3.4 anomaly is +2.5 °C for July–September and the twelve prediction systems used here project +3.8 °C for December–February, in line with the NOAA, IRI and WMO outlooks. The Dipole Mode Index (DMI) is +0.2 °C for July–September, below the +0.4 °C event threshold, and the models return it to neutral by January–March.

The forecast. Both outlooks are candidate C of the objective forecast: the equal-weight combination of three statistical components, canonical correlation analysis, logistic regression on the ocean indices and the smoothed-coefficient regression of Kharin et al. (2017), hereafter Kharin, chosen among five stated combinations of five components by its cross-validated skill over 1991–2020 (the Method section). Every map issues a category only where that hindcast scores at least as well as climatology in the cell (a ranked probability skill score, RPSS, of 0 or more); the cells that fail are left white, the same as a cell with no category above 40 %, so white over land means either.

Ocean state

At issuance the equatorial Pacific is in a strong El Niño. The observed Niño3.4 anomaly for July–September 2026 is +2.5 °C. The twelve models project a mean anomaly of +3.9 °C for November–January, +3.8 °C for December–February and +3.4 °C for January–March, with a model range of +2.8 to +4.8 °C in December–February. They place the peak in November–January and keeps the anomaly above +3 °C through January–March. The DMI is +0.2 °C for July–September in the ERSSTv5 record (Huang et al., 2017), below the +0.4 °C event threshold. The Bureau of Meteorology's weekly index has been above the threshold for five weeks without an event being declared. The

models return the DMI to neutral through the season, +0.6 °C in November–January, +0.3 °C in December–February and 0.0 °C in January–March.

The models and the published outlooks (NOAA CPC, 2026; IRI, 2026; WMO, 2026; Bureau of Meteorology, 2026; Table 1) agree on both drivers. The models' Niño3.4 of +3.8 °C for December–February is above WMO's +3.7 °C for October–December and above the +2.5 °C that CPC gives as the threshold of a historic event. CPC's +2.1 °C is a weekly value on a different dataset and is not comparable with the seasonal ERSST value used here. The DMI evolution matches WMO's peak in October followed by decline. In the models the DMI is above its threshold in November–January only, and the El Niño persists through all three seasons.

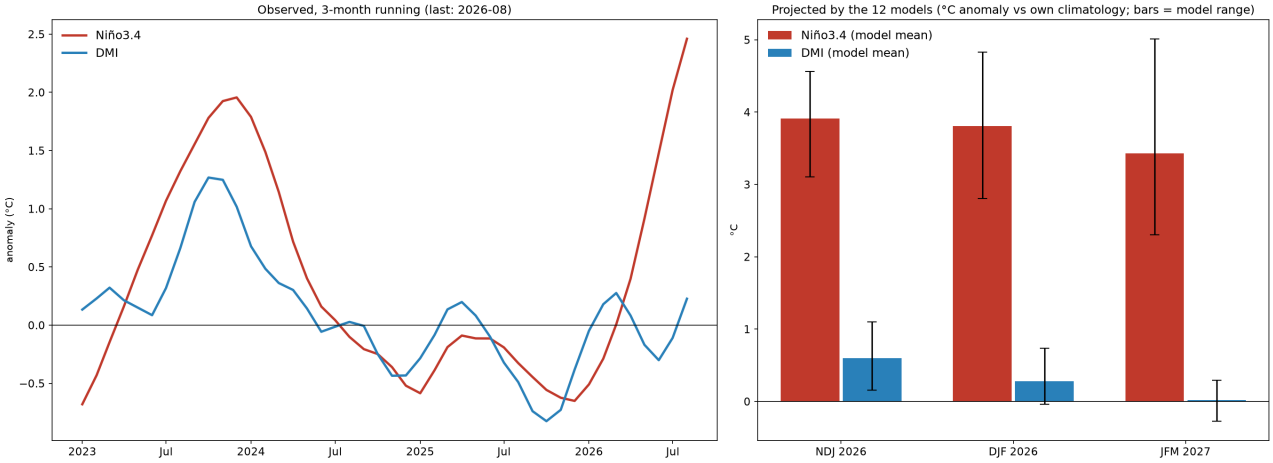


Figure 1: Observed Niño3.4 and DMI, three-month running anomalies against 1991–2020 (left), and the twelve models' mean and range for each target season from the October 2026 initialisations, as anomalies against each model's own climatology (right).

Table 1: Published ocean outlooks at issuance, with their issue dates. The Bureau of Meteorology value is relayed by secondary sources, not fetched directly.

source	issued	outlook
NOAA CPC, ENSO diagnostic discussion	8 Oct 2026	El Niño Advisory. Niño3.4 +2.1 °C (weekly). "A strong-to-very strong El Niño likely through January–March 2027"; "chances remain high for a historic event (+2.5 °C or more)"
IRI / CPC probabilistic ENSO outlook	21 Sep 2026	El Niño 100 % for every season from SON 2026 to FMA 2027. "Numerous models project Niño3.4 values that could reach or exceed +3.0 °C"
WMO Global Seasonal Climate Update	8 Oct 2026	Niño3.4 "approximately +3.7 °C during OND 2026", "peaking around December 2026". Positive IOD "predicted to peak in October 2026 and then decline", OND mean +0.5 °C
Australian Bureau of Meteorology, weekly IOD index	11 Oct 2026	+0.88 °C, fifth consecutive week above the +0.4 °C threshold, status neutral pending sustained values

The four past years whose Niño3.4 and DMI evolution over the twelve seasons to July–September most resembles this year's are 1997 (correlation 0.91), 2023 (0.83), 2002 (0.82) and 1990 (0.68). 1997 and 2023 were strong El Niño years with a positive DMI. Two of the four, 1997 and 2002, fall inside the 1991–2020 record. In December–February 1997/98 the season was wet over equatorial East Africa, Angola and Zambia, and dry over Botswana, Mozambique and Zimbabwe. The analogue component of the forecast uses the ten closest years, not these four. The notebook plots the twelve-season evolution of both indices for this year against the four.

Rainfall outlook

The objective forecast for December–February 2026/27 is candidate C, the equal-weight combination of canonical correlation analysis, logistic regression on the ocean indices and Kharin (Key messages). Its cross-validated skill over the land cells in season, 1991–2020, is a generalised relative operating characteristic score (GROC, 0.5 is no skill) of 0.598 and an RPSS (0 is climatology) of 0.040 (Table 2). Figure 2 issues a category only where the cell's own cross-validated RPSS is at least 0. The 38 % of land cells in season that fail are white, as are the cells with no category above 40 %, and the box averages below are over the cells kept.

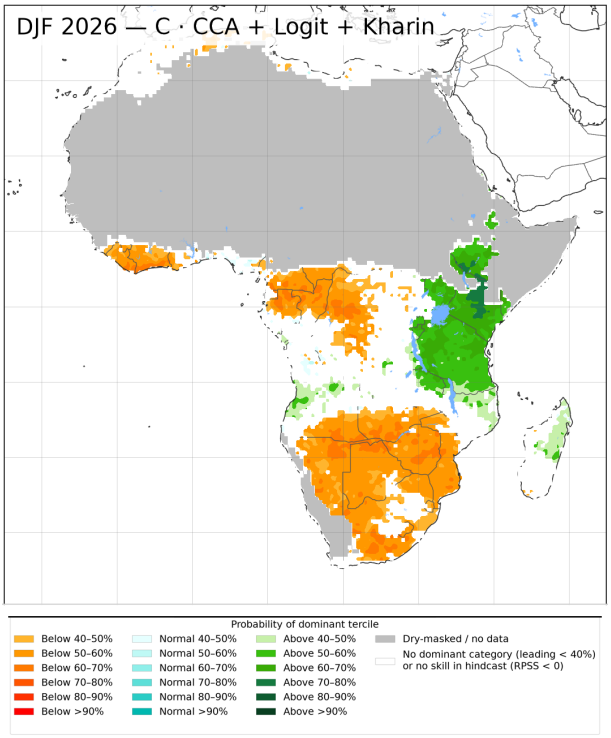


Figure 2: Rainfall, December–February 2026/27, from the October 2026 initialisations. Objective forecast, candidate C (CCA + logistic regression + Kharin). Probability of the dominant tercile. Grey is dry season, white over land is no category above 40 % or no skill in the hindcast (RPSS below 0).

Equatorial East Africa. Above-normal rainfall at 60 to 70 % over Kenya, southern Somalia, northern Tanzania and Uganda, 70 to 80 % over central and eastern Kenya, and 50 to 60 % over southern Ethiopia and northern Kenya. Almost every cell of the East African box is kept, and its above-normal average is 62 %.

Southern Africa. Below-normal rainfall at 50 to 70 % over Botswana, Zimbabwe, Namibia, the South African interior, southern Angola and southern Mozambique, highest over Botswana, Zimbabwe and the South African interior. The box average for the below-normal category is 54 % over the 88 % of its cells kept. About half of Angola, Zambia and northern Mozambique is white for lack of skill. Of the cells kept there, Zambia leans below-normal and northern Mozambique above-normal, mostly in the 40 to 50 % band.

Central and West Africa. Below-normal rainfall at 50 to 70 % over Cameroon, Gabon and the Congo coast, and at 40 to 60 % along the Guinea coast from Sierra Leone to southern Nigeria. Two thirds of the cells in both regions pass the RPSS criterion. The interior Congo basin is white for lack of skill over half of its cells, and the components disagree over Central Africa.

Madagascar, the Sahel and North Africa. Madagascar is white for lack of skill over two thirds of its cells, and where it is kept the above-normal category leads at 40 to 50 %. The Sahel is in its dry season and is masked. The Maghreb coast is white for lack of skill over four fifths of its cells, and the rest carries below-normal rainfall at 40 to 50 %.

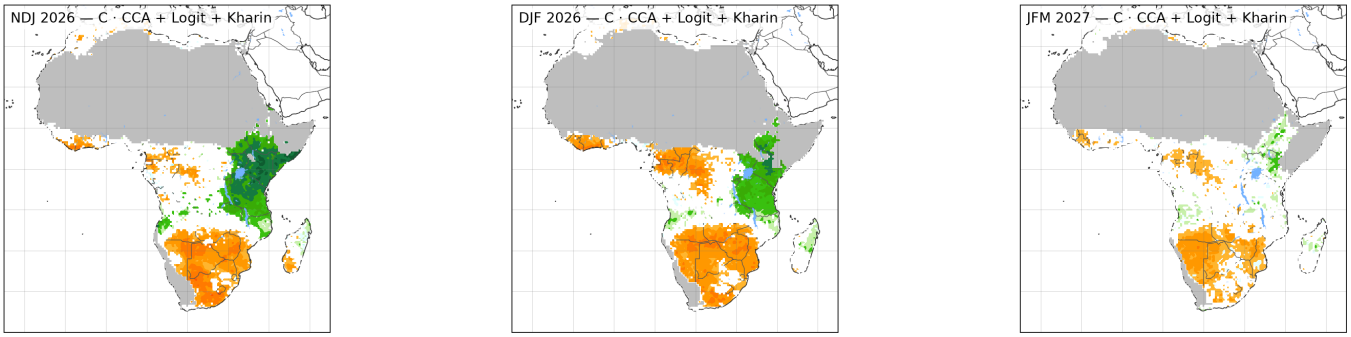


Figure 3: Rainfall, November–January, December–February and January–March 2026/27, from the October 2026 initialisations. Objective forecast for each season, candidate C, the no-skill cells of each season white. Legend as in Figure 2. Panel labels give the year the season starts, so DJF 2026 is December 2026 to February 2027.

Candidate C is the best-scoring candidate in all three seasons among those built on the two ocean indices (Table 2). The RPSS criterion keeps 57 % of the land cells in season for November–January, 62 % for December–February and 45 % for January–March. The probabilities are highest in November–January. Above-normal rainfall reaches

70 to 90 % over Kenya, Tanzania and Uganda, with a box average of 72 %, and below-normal rainfall averages 54 % over the southern African box. By January–March the East African box average for above-normal rainfall falls to 43 % and 43 % of that box is white for lack of skill, and much of southern Africa drops to the 40 to 50 % band for below-normal, with Botswana and Zimbabwe the cells that still carry a clear below-normal lean. For every candidate the cross-validated skill is lower for January–March than for the other two seasons.

Temperature outlook

The objective forecast for December–February 2026/27 is candidate C, with a cross-validated GROC of 0.688 and an RPSS of 0.142 on the continental mean (Table 3). The tercile thresholds are drawn from 1991–2020, and the continent has warmed through that period, so a season near the mean of recent years sits in the upper tercile before any seasonal signal is added. All twelve models forecast a warm anomaly almost everywhere against their own climatologies. Figure 4 leaves white the 10 % of land cells whose cross-validated RPSS is below 0, mainly Mauritania and the western Sahara, with scattered cells in the Sahel, Egypt and on the Namibian coast. The box averages below are over the cells kept.

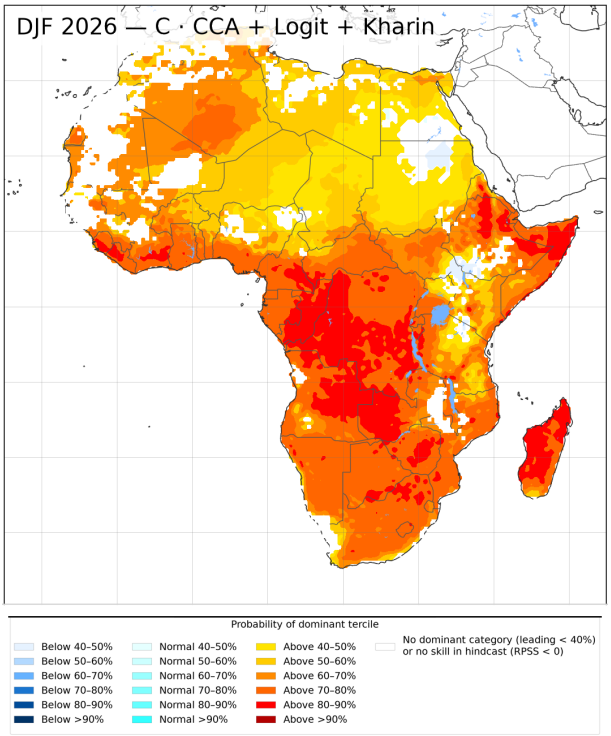


Figure 4: 2 m temperature, December–February 2026/27, from the October 2026 initialisations. Objective forecast, candidate C. Probability of the dominant tercile, below-normal, near-normal or above-normal. White over land is no category above 40 % or no skill in the hindcast (rpss below 0).

Central, southern and eastern Africa. Above-normal temperature at 80 to 90 % over Angola, Madagascar, Mozambique, Somalia, Tanzania and Zambia, the Congo basin and the Ethiopian highlands, and at 60 to 80 % over Botswana, Namibia, South Africa and Zimbabwe. The above-normal box averages are 75 % for southern Africa and 64 % for East Africa.

West Africa, the Sahel and North Africa. Above-normal temperature at 70 to 80 %, locally 80 to 90 %, along the Guinea coast, and at 40 to 60 % over Egypt, the Maghreb, the Sahara and the Sahel. The Sahel box average for above-normal is 53 %.

Nile valley and Lake Victoria basin. Over the Nile valley from northern Sudan into Egypt, the Lake Victoria basin and the Kenyan highlands, no category reaches 50 %. Below-normal temperature leads at 40 to 50 % over northern Sudan and around Lake Victoria. Both come from the logistic-regression component, whose Niño3.4 fits give below-normal temperature over equatorial East Africa and the eastern Sahara under a strong El Niño, with little contribution from the DMI fits. In these regions the seasonal signal opposes the warming trend.

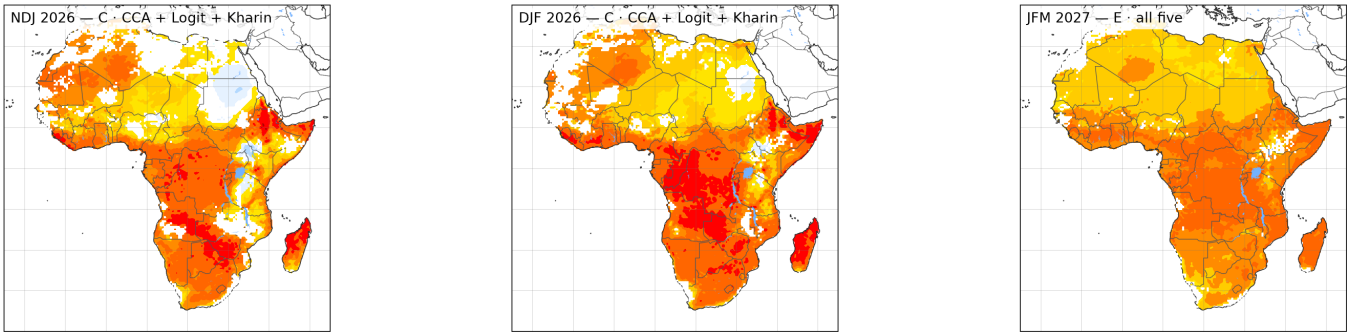


Figure 5: 2 m temperature, November–January, December–February and January–March 2026/27, from the October 2026 initialisations. Objective forecast for each season, the no-skill cells of each season white. Legend as in Figure 4.

Candidate C is the best-scoring candidate for November–January and December–February. For January–March

candidate E, which adds the ensemble regression and the analogue frequency, scores 0.691 against 0.680 for C (Table 3). The spatial pattern is the same in all three seasons. The continental mean of the above-normal probability over the cells kept is 61 % in November–January, 65 % in December–February and 62 % in January–March. The RPSS criterion blanks 15, 10 and 5 % of the land cells, in November–January mostly over Egypt and Libya. In January–March West Africa and the western Sahel reach the 60 to 70 % band and the East African area of no dominant category contracts.

How the forecast is made

The forecast is built from twelve seasonal prediction systems, six from the North American Multi-Model Ensemble (NMME; Kirtman et al., 2014) and six from the Copernicus Climate Change Service seasonal archive (C3S, 2026), all initialised in October 2026 (Table 4). Three fields are taken from each system for each target season, the global sea surface temperature (SST), the tropical-band rainfall or 2 m temperature, and the African rainfall or 2 m temperature. Rainfall is verified against CHIRPS v2 (Funk et al., 2015) and temperature against ERA5 (Hersbach et al., 2020), both aggregated to the target season on a 0.5° grid over 1991–2020, which is also the period that defines the tercile categories.

Five components turn these inputs into tercile probabilities. Canonical correlation analysis (CCA) relates African rainfall or temperature to three predictor sets, namely the observed SST of the month before initialisation, each model's forecast SST, and each model's forecast of the target variable. There is one fit per model and predictor domain, with the number of modes chosen objectively inside every cross-validation fold. Predictand cells in their dry season (under 50 mm in the season on average) are removed before the fit, as CPT's dry mask does in ACMAD's workflow; the other four components are fitted cell by cell, so the mask does not enter them. A logistic regression relates each cell's tercile to the Niño3.4 and DMI values taken from each model's forecast SST. An ensemble regression calibrates each model's forecast of the target variable cell by cell and carries the ensemble spread into the probabilities. Kharin fits a regression of the observations on each model's ensemble mean for all twelve seasons at this lead time and smooths the coefficients across neighbouring seasons, for the four systems with monthly initialisations. The analogue component selects the ten past years whose Niño3.4 and DMI evolution most resembles this year's and takes the share of those years that fell in each tercile.

Candidates, lettered A to E, are equal-weight combinations of subsets of the components. Every component and candidate carries a hindcast over 1991–2020 in which each year is forecast with that year and its two neighbours on either side held out of training. The candidate with the highest cross-validated GROC for a season is the objective forecast for that season. Maps follow the RCC Climate Forecast Colormap Palettes, with six probability bands from 40 % and no colour where the dominant category is below 40 %. A category is issued only where the candidate's own cross-validated RPSS over 1991–2020 is at least 0; the cells below that are white on every map, like the cells with no dominant category, and are left out of the box averages. In the figure labels the components are CCA, Logit (the logistic regression, Logit4 with four indices), eReg (the ensemble regression), Kharin and Analogues. Candidate C is CCA + Logit + Kharin, C4 the same with Logit4, and E all five.

Verification

Where the forecast has skill

The issued maps apply one criterion. A cell is kept where the candidate's cross-validated RPSS is at least 0, and is white where it is below, worse than issuing climatology, so white over land means no dominant category or no skill. For December–February rainfall that removes 38 % of the land cells in season: about half of the Congo basin interior, Angola and Zambia, two thirds of Madagascar, four fifths of the Maghreb coast, and 12 % of the southern African box against 2 % of the East African box. The looser criterion, a GROC below 0.5, no discrimination between wetter and drier years, removes 21 %, concentrated in the same places. Figure 6 shows the forecast with no mask and with the GROC criterion, so that what the issued map leaves out can be seen. The notebook also draws both criteria hatched. For temperature the RPSS criterion removes 10 % of the land cells for December–February.

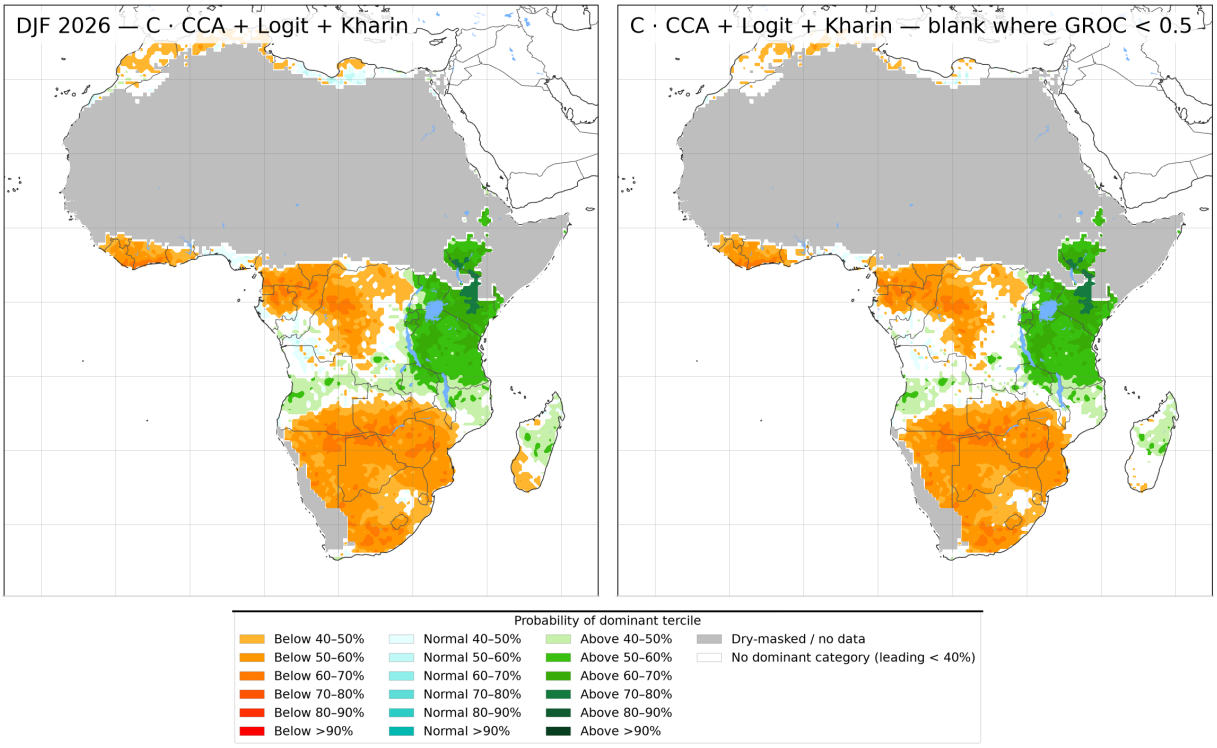


Figure 6: Rainfall, December–February 2026/27, candidate C, with no skill criterion applied (left) and with the cells of cross-validated GROC below 0.5 left blank (right). Hindcast 1991–2020. The issued map, Figure 2, applies the RPSS criterion.

Candidate ranking and reliability

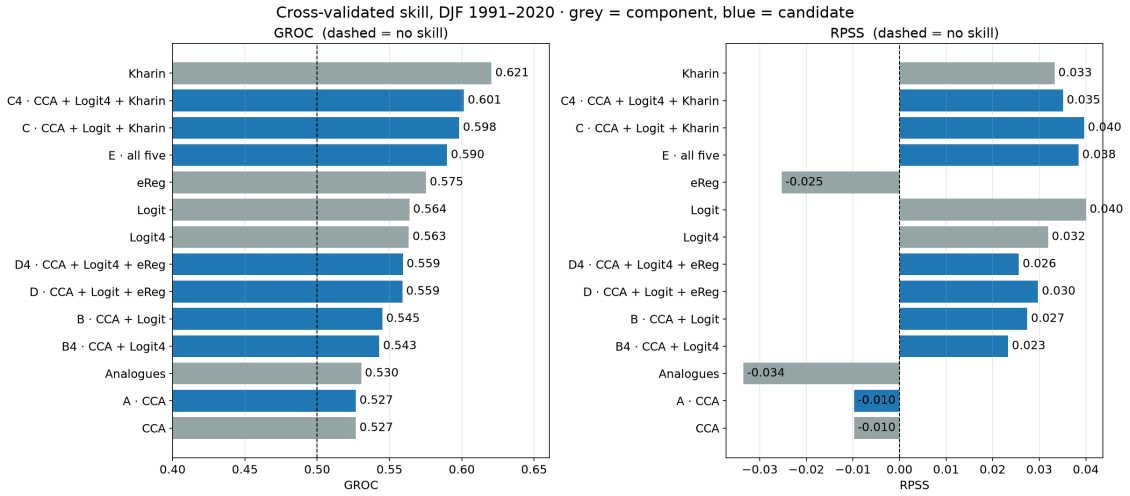


Figure 7: Rainfall, December–February 2026/27. Cross-validated GROC and RPSS of every component (grey) and candidate (blue), hindcast 1991–2020.

All scores are leave-years-out cross-validated over 1991–2020, with the forecast year and its two neighbours on either side held out of every fit, and are means over the continent's land cells, the dry-season cells excluded for rainfall. The record is 29 years for November–January and December–February and 30 for January–March (28 for Kharin), so differences of a few hundredths between candidates are within sampling uncertainty.

For rainfall, candidate C is the best candidate in each season (Table 2). Kharin, fitted on the four systems with monthly initialisations, is the best single component (0.621 for December–February). The logistic regression (0.564) and the ensemble regression (0.575) follow, and the CCA on its own scores 0.527. The logistic regression and Kharin are the components with a positive RPSS. The cell-by-cell GROC is 0.6 to 0.8 over Botswana, Mozambique, South Africa and Zimbabwe and over Kenya and Tanzania, and shows no skill over Angola, Madagascar and the

Congo basin (Figure 6).

For temperature every December–February candidate scores between 0.64 and 0.69, with candidate C at 0.688 and an RPSS of 0.142. The ensemble regression (0.699) and Kharin (0.691) are the highest-scoring components. The logistic regression scores 0.554 and the analogue frequency 0.458, below the no-skill value of 0.5. The cell-by-cell GROC is 0.7 to 0.9 over the Congo basin, the tropics, southern Africa and Madagascar and 0.5 to 0.7 over the Sahara and the Maghreb. The reliability diagrams (Figure 8) show the temperature candidate under-confident, its curve steeper than the diagonal. The rainfall candidate is over-confident in the 40 to 70 % range for all three categories, and only its highest above-normal bin lies on the diagonal.

Table 2: Rainfall: the best candidate for each season, its regional box averages over the cells kept (%, East Africa 5° S–12° N, 33–52° E; southern Africa 30–15° S, 15–35° E), its cross-validated skill over every land cell in season, and the share of those cells the RPSS criterion keeps.

season · candidate	east Africa P(above)	southern Africa P(below)	southern Africa P(above)	GROC	RPSS	kept %
NDJ · C	72	54	14	0.590	0.041	57
DJF · C	62	54	17	0.598	0.040	62
JFM · C	43	48	21	0.541	0.005	45

Table 3: Temperature: the best candidate for each season, its regional box averages over the cells kept (%, the same boxes, Sahel 10–18° N, 15° W–30° E), its cross-validated skill over every land cell, and the share of cells kept.

season · candidate	continent P(above)	east Africa P(above)	southern Africa P(above)	Sahel P(above)	GROC	RPSS	kept %
NDJ · C	61	59	74	49	0.660	0.113	85
DJF · C	65	64	75	53	0.688	0.142	90
JFM · E	62	66	64	58	0.691	0.152	95

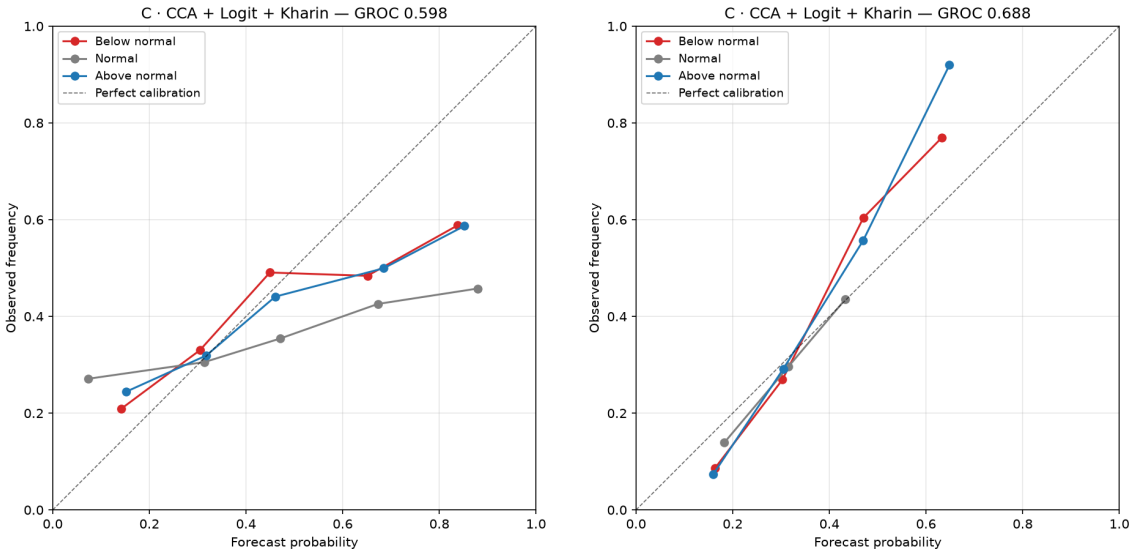


Figure 8: Reliability diagrams of candidate C for rainfall (left) and 2 m temperature (right), December–February 2026/27, hindcast 1991–2020.

Limitations

The tercile categories are fixed on 1991–2020 and the continent has warmed through that period, so the temperature probabilities carry the trend as well as the seasonal signal. The ocean-state components show where the two differ.

The twelve systems have hindcasts of unequal length. Three end before 2020, and every method is fitted on each system's own years rather than on a common window. Of the two components driven by the ocean indices, the analogue frequency has no skill for temperature and the logistic regression has a GROC of 0.554. Half of the temperature logistic regression's DMI fits fail its minimum-data checks, so its output comes mainly from the Niño3.4 fits. One system, CFSv2, has no data over north-west Africa in its African rainfall and temperature fields, so the ensemble regression and the candidates that contain it are eleven-model products over the Maghreb and the western Sahel. No system was excluded this cycle. The two with the lowest cross-validated skill, CCSM4 (0.495) and GEOSS2S (0.505), sit at the no-skill line, and the per-model skill maps in the notebook are the basis for any exclusion in a later cycle.

Blanking the cells of negative RPSS removes a third of the rainfall map in December–February and over half in January–March. The criterion is a 29-year cross-validated score on single cells and is noisy: a cell can fail by a small margin and its neighbour pass, and the GROC criterion keeps more. The blanked cells carry a forecast in the saved fields, so ACMAD can issue them under its own rule.

The published ocean outlooks are quoted as issued.

References

Bureau of Meteorology, 2026: Climate driver update, weekly Indian Ocean Dipole index, 11 October 2026. http://www.bom.gov.au/climate/enso/

C3S, 2026: Seasonal forecast monthly statistics and daily data on single levels. Copernicus Climate Change Service, Climate Data Store. https://cds.climate.copernicus.eu

Funk, C., P. Peterson, M. Landsfeld, D. Pedreros, J. Verdin, S. Shukla, G. Husak, J. Rowland, L. Harrison, A. Hoell and J. Michaelsen, 2015: The climate hazards infrared precipitation with stations: a new environmental record for monitoring extremes. *Scientific Data*, 2, 150066. https://doi.org/10.1038/sdata.2015.66

Hersbach, H., and co-authors, 2020: The ERA5 global reanalysis. *Quarterly Journal of the Royal Meteorological Society*, 146, 1999–2049. https://doi.org/10.1002/qj.3803

Huang, B., P. W. Thorne, V. F. Banzon, T. Boyer, G. Chepurin, J. H. Lawrimore, M. J. Menne, T. M. Smith, R. S. Vose and H.-M. Zhang, 2017: Extended Reconstructed Sea Surface Temperature, version 5 (ERSSTv5): upgrades, validations, and intercomparisons. *Journal of Climate*, 30, 8179–8205. https://doi.org/10.1175/JCLI-D-16-0836.1

IRI, 2026: ENSO forecast, probabilistic outlook issued 21 September 2026. International Research Institute for Climate and Society, Columbia University. https://iri.columbia.edu/our-expertise/climate/forecasts/enso/current/

Kharin, V. V., W. J. Merryfield, G. J. Boer and W.-S. Lee, 2017: A postprocessing method for seasonal forecasts using temporally and spatially smoothed statistics. *Monthly Weather Review*, 145, 3545–3561. https://doi.org/10.1175/MWR-D-16-0337.1

Kirtman, B. P., and co-authors, 2014: The North American Multimodel Ensemble: phase-1 seasonal-to-interannual prediction; phase-2 toward developing intraseasonal prediction. *Bulletin of the American Meteorological Society*, 95, 585–601. https://doi.org/10.1175/BAMS-D-12-00050.1

NOAA CPC, 2026: ENSO diagnostic discussion, 8 October 2026. NOAA Climate Prediction Center, College Park. https://www.cpc.ncep.noaa.gov/products/analysis_monitoring/enso_advisory/ensodisc.shtml

WMO, 2026: Global Seasonal Climate Update, issued 8 October 2026. World Meteorological Organization, Geneva. https://wmo.int/resources/publication-series/global-seasonal-climate-update

Appendix

Table 4: The twelve prediction systems.

model	product	hindcast	members
CCSM4	nmme/ccsm4	1991–2020	10
CESM1	nmme/cesm1	1991–2020	10
CFSv2	nmme/cfsv2	1991–2011	24
CMCC	c3s/cmcc-sps4	1993–2020	30
CanSIPS-IC4	nmme/cansipsic4	1991–2020	40
CanSIPSv3	c3s/eccc-cansipsv3	1993–2020	20
DWD	c3s/dwd	1993–2020	30
ECMWF	c3s/ecmwf-monthly	1991–2016	25
GEOSS2S	nmme/geoss2s	1991–2017	4
JMA	c3s/jma-cps4	1993–2020	10
Meteo-France	c3s/meteofrance	1993–2020	31
SPEAR	nmme/spear	1991–2020	15

Table 5: Per-model cross-validated skill of the ensemble regression, December–February 2026/27, hindcast 1991–2020.

model	rainfall GROC	rainfall RPSS	temperature GROC	temperature RPSS
CCSM4	0.495	−0.117	0.639	0.066
CESM1	0.532	−0.072	0.647	0.079
CFSv2	0.532	−0.080	0.656	0.126
CMCC	0.553	−0.046	0.640	0.064
CanSIPS-IC4	0.573	−0.020	0.695	0.169
CanSIPSv3	0.552	−0.054	0.638	0.080
DWD	0.518	−0.086	0.556	−0.046
ECMWF	0.566	−0.028	0.677	0.131
GEOSS2S	0.506	−0.098	0.612	0.040
JMA	0.511	−0.084	0.626	0.072
Meteo-France	0.533	−0.065	0.652	0.110
SPEAR	0.523	−0.079	0.614	0.043

Table 6: Settings of the issued run. Record, cross-validation and ranking are given in the Method section. The notebooks' first code cell holds every value.

setting	value
initialisation and targets	October 2026 for NDJ 2026, DJF 2026/27 (primary) and JFM 2027
domain and grid	the African continent, 40° S–40° N, 25° W–55° E, 0.5°
rainfall predictand	CHIRPS v2 monthly, seasonal mean; cells with under 50 mm in the season on average are a dry season and are masked
temperature predictand	ERA5 2 m temperature, seasonal mean
CCA	three predictor sets (observed SST of the month before initialisation, model SST, model target field); modes by the Scree test and North's rule in every fold
logistic regression	Niño3.4 and the DMI from each model's forecast SST; the four-index variant adds the SAOD and the SWIO
ensemble regression	per cell, per model, ensemble spread carried into the probabilities; negative rainfall clipped
Kharin (smoothed-coefficient regression)	the four systems with monthly initialisations; coefficients smoothed across neighbouring seasons; gamma distribution for rainfall, normal for temperature
analogues	the ten past years closest in the twelve-season evolution of Niño3.4 and the DMI, re-selected in every fold